

A “pulsational” distance determination for the Large Magellanic Cloud¹

Marcella Marconi

*INAF - Osservatorio Astronomico di Capodimonte, via Moiarello 16, I-80131 Napoli, Italy.
email: marcella@na.astro.it*

Gisella Clementini

*INAF - Osservatorio Astronomico di Bologna, Via Ranzani 1, I-40127 Bologna, Italy. email:
gisella.clementini@bo.astro.it*

ABSTRACT

We present results from the theoretical modelling of the observed B, V light curves of 14 RR Lyrae stars in the Large Magellanic Cloud. The sample includes 7 fundamental and 7 first overtone pulsators covering the metallicity range from -2.12 to -0.79 dex in $[\text{Fe}/\text{H}]$, with average value of -1.54 dex. Masses, intrinsic luminosities, effective temperatures, and reddenings were derived by fitting high accuracy multiband light curves available for these RR Lyrae stars to nonlinear convective pulsation models. Individual distance moduli were determined for each variable, they lead to an average distance modulus for the Large Magellanic Cloud of $\mu_0 = 18.54 \pm 0.02$ ($\sigma = 0.09$ mag, standard deviation of the average), in good agreement with the “long” astronomical distance scale.

Subject headings: Stars: evolution - stars: horizontal branch - stars: variables: RR Lyrae - LMC

1. INTRODUCTION

One of the most debated issue of modern astrophysics is the definition of the local distance scale and of the distance of its first step, the Large Magellanic Cloud (LMC), in particular. Indeed, current calibrations of the extragalactic distance scale and consequent evaluations of the Hubble constant rely upon the Classical Cepheid PL relations with the zero point fixed by some assumption on the LMC distance (see e.g. Freedman et al. 2001, Tammann, Sandage, & Reindl 2003). Recent determinations of the LMC distance modulus, either based on Population I or II distance indicators, cover the range 18.3-18.7 mag (see discussions in Cacciari 1999, Walker 1999, Carretta et al. 2000,

¹Based on observations collected at the European Southern Observatory, proposals 62.N-0802, 66.A-0485, and 68.D-0466

Caputo et al. 2000). However, in the last couple of years different distance indicators have followed the trend to converge to a common value of $\mu_{LMC}=18.52 \pm 0.02$ mag, on the basis of updated accurate photometric data for both RR Lyrae and red clump stars, as well as revised techniques and consistent reddening evaluations (see discussions in Clementini et al. 2003, hereinafter C03, Walker 2003, and Alves 2004).

Among the different methods exploiting the radially pulsating stars as standard candles a quite innovative and promising technique is represented by the fitting of the observed light and radial velocity curves of a pulsating star to those predicted by nonlinear pulsation models (see e.g. Wood, Arnold & Sebo 1997, hereinafter WAS; Keller & Wood 2002; Bono, Castellani, & Marconi 2000, 2002, hereinafter BCM00 and BCM02, respectively; Di Fabrizio et al. 2002). This technique is based on the direct comparison between observed and predicted curves, rather than involving related parameters such as pulsation amplitudes and Fourier parameters, and performs the theoretical reproduction of both general features (period, shape, amplitude) and morphological details such as bumps and humps, of the observed curves. Given the sensitivity of the curve detailed morphology to the model input parameters, as well as to the physical and numerical assumptions, the fitting of actual light and radial velocity curves offers a unique opportunity to obtain sound estimates of the intrinsic stellar properties of the variables, providing at the same time a key test of the theoretical predictions.

High accuracy observational data, consisting of well sampled multiband light and, possibly, radial velocity curves, knowledge of the related pulsation characteristics, namely period, colors and amplitudes, and of the metallicity of the variable star, are needed for a meaningful application of the method. The output of the procedure is a set of models for fixed period and metal abundance and with varying the mass, the luminosity and the effective temperature¹, among which the best fitting model is that best reproducing the observed characteristics of the pulsation, within acceptable values of the derived intrinsic parameters.

In the case of variables of RR Lyrae type this technique has already provided very good results for Galactic field first overtone RR Lyrae stars (see BCM00, Di Fabrizio et al. 2002), whereas for the fundamental mode pulsators satisfactory results were obtained except for the long period variables close to the red edge of the RR Lyrae instability strip (see Castellani, Degl’Innocenti, & Marconi 2002, Di Criscienzo, Marconi, & Caputo 2004).

As for the Classical Cepheids a similar technique was early applied by WAS to the LMC bump Cepheid HV905. More recently, relying on the same theoretical pulsational scenario as in BCM00, the method was applied to two LMC fundamental mode Cepheids showing well-defined bumps along the decreasing (short-period) and the rising (long-period) branch of the light curve, respectively (BCM02), based on data from the OGLE catalogue (available at sirius.astrouw.edu.pl/~ogle/ogle2/dia).

¹We note that mass, luminosity and effective temperature are not independent variables because of the existence of a Period-Density relation for pulsating stars.

A good fit was obtained for both variables and for an LMC distance modulus ranging from 18.48 to 18.58 mag (see BCM02 for details), in agreement with results by C03. An independent application to the MACHO V and R light curves of 20 *bump* Cepheids in the LMC (including HV905) was performed by Keller & Wood (2002), on the basis of the WAS nonlinear pulsation code. They obtained a mean LMC distance modulus of 18.55 ± 0.02 (intrinsic error of the average).

Both in the case of RR Lyrae stars and Classical Cepheids the best fit models based on BCM00 theoretical scenario seem to suggest that the standard value of the mixing length parameter ($l/H_p = 1.5$) adopted to close the dynamical-convective equation system is suitable to reproduce the light variations of variables in the blue region of the instability strip. A higher value of l/H_p is needed instead toward the red region of the fundamental mode instability strip (see e.g. BCM02). This occurrence is confirmed by results based on other independent “pulsational” methods to constrain the RR Lyrae and globular cluster distance scale, in particular the Period-Amplitude relations and the comparison in the Period-Magnitude diagram (see Di Criscienzo et al. 2004).

In this paper we present results from the theoretical modelling of the observed B, V light curves of 14 RR Lyrae stars in the LMC, based on the detailed photometric study of the LMC RR Lyrae stars by C03 and Di Fabrizio et al. (2004, hereinafter DF04). Our sample includes 7 fundamental mode (RRab) and 7 first overtone (RRc) pulsators that, according to Gratton et al. (2004, hereinafter G04) spectroscopic analysis, cover the metallicity range from -2.12 to -0.79 in $[\text{Fe}/\text{H}]$, with average value of -1.54 dex. The application of the method to a significant number of Population II pulsators in the same stellar system, namely the LMC RR Lyrae stars, represents a powerful test of the inner consistency and predictive capability of the adopted theoretical scenario, providing at the same time an independent estimate of the LMC distance modulus, and a direct comparison between Population I and II distance indicators, which contributes to strengthen our knowledge of the local distance scale.

The organization of the paper is the following. In Sect. 2 we briefly discuss the adopted photometric (light curves and reddening values) and spectroscopic (metallicities) databases. In Sect. 3 we present the pulsation models, whereas the fit of the observed light curves and the derivation of the intrinsic stellar parameters (masses, luminosities, and effective temperatures) both for fundamental and first overtone pulsators is described in Sect. 4. In this section we also discuss the comparison with the intrinsic parameters predicted for the program stars by the evolutionary horizontal branch (HB) models, and by the Fourier decomposition of the visual light curves of the fundamental mode RR Lyrae stars. The derived LMC distance modulus and the associated uncertainty are presented in Sect. 5 along with a discussion of the resulting RR Lyrae luminosity-metallicity relation. A summary of the results and some final remarks in Section 6 close the paper.

2. THE OBSERVATIONAL DATABASE

The RR Lyrae stars analyzed in the present paper were selected from the high quality photometric catalogue of variable stars in the LMC published by DF04. The catalogue contains B, V, I light curves in the Johnson-Cousins photometric system of 162 variables located in two areas (referred to as Field A and B) close to the bar of the LMC, among which 135 are RR Lyrae stars. These variables were used by C03 to very carefully determine the distance of the LMC, getting the value $\mu_0(LMC)=18.515 \pm 0.085$ mag (1σ scatter of the mean) as the average of 17 independent methods based both on Population I and II distance indicators. A large fraction of the RR Lyrae stars in DF04 were also analyzed spectroscopically by G04 who measured individual metal abundances for about a hundred of them, using low resolution spectra taken with FORS at the VLT.

The target stars were selected by visual inspection of DF04 catalogue, preferring objects with well sampled and accurate light curves, and variety of morphologies, periodicities, and colors. We chose for our analysis a number of single-mode fundamental and first overtone pulsators not affected by Blazhko effect (Blazhko 1907) or other irregularities of the light variations. The selected objects all have evenly covered B, V light curves with about 60-70 data points in V and about 40 in B , and with internal photometric accuracy of 0.02-0.04 mag in V and 0.03-0.05 mag in B , according to DF04. The I light curves in DF04 catalogue are generally of lower accuracy and have a rather limited number of data-points (14-15), thus we did not attempt the fit in this band.

To ensure variety of the light curve morphologies we selected objects spanning a range in period: from 0.487 to 0.656 days for the fundamental mode, and from 0.232 to 0.385 days for the first overtone pulsators.

Metallicities $[Fe/H]$ are available for all our targets, either from the spectroscopic analysis by G04, or estimated according to Jurcsik and Kovács (1996) method from the ϕ_{31} parameter of the Fourier decomposition of the visual light curves (see Sections 6 and 6.1 of DF04). G04 spectroscopic metal abundances are tied to the metallicity scale defined by Harris (1996) $[Fe/H]$ abundance for the galactic globular clusters M 68 and NGC 1851 (see Section 4 in G04), on average they are 0.06 more metal-rich than the Zinn & West (1984) scale. The “photometric” metallicities (star #9660, only) were transformed to G04 scale according to the procedure described in Section 3.3 of C03. The metallicity range spanned by the selected targets (from -2.12 to -0.79 dex in $[Fe/H]$ in G04 scale) is large enough to allow the check of the luminosity-metallicity relation of the LMC RR Lyrae derived by other studies (e.g. C03 and G04) using the absolute magnitudes derived from the model fitting (see Section 5.1).

Following the selection criteria described above, we ended up having in our sample a number of RRab’s with relatively long period ($P > 0.6$ days). One of them (star # 9660) also has relatively high metal abundance ($[Fe/H]=-1.5$) and, as confirmed by its rather red color ($< B - V >=0.47$

mag), lies close to the red edge of the RR Lyrae instability strip². This is the object for which we have achieved the least satisfying model fitting (see Section 4 and Fig. 1). Indeed, as anticipated in the Introduction, current pulsation models often fail to reproduce the morphology of the light curves of long period fundamental mode RR Lyrae stars close to the FRE. In fact, while the theoretical light curves are generally able to reproduce the saw-like shape with amplitude decreasing from the FBE to the FRE of the observed fundamental mode RR Lyrae stars, at the lowest effective temperatures the models also show a secondary peak before the phase of maximum light. This secondary peak is of increasing strength as the FRE is being approached. However, it is not present in the observed light curves.

C03 estimated the average reddening of the LMC fields containing our targets using the colors of the edges of the RR Lyrae instability strip. They derived $E(B - V) = 0.116 \pm 0.017$ for the field closer to the LMC bar (Field A), and $E(B - V) = 0.086 \pm 0.017$ mag for the more external one (Field B), corresponding to a differential reddening of 0.03 mag between the two areas. Our RRc sample includes two of the 3 variables that define the first overtone blue edge (FOBE) of the RR Lyrae stars in C03 and DF04. C03 also estimated individual reddenings for the RRab variables using the Sturch (1966) method, which is based on the mean $\langle B - V \rangle$ colors at minimum light of the variables. The color excesses inferred from our model fitting procedure can be directly compared with both average and individual reddenings in C03, thus providing an independent check of C03 values, hence of the distance for the LMC in that paper. This check is particularly relevant in light of the controversy existing on the actual reddening towards the LMC (see discussions in Udalski et al. 1999, hereinafter U99; Zaritsky 1999; C03; Alcock et al. 2004, hereinafter A04; Zaritsky et al. 2004) and is presented in Section 4.4.

The list of RR Lyrae stars analyzed in the paper is provided in Table 1 along with a summary of their relevant observed quantities. Namely we list: identifier, variable type and period, intensity-averaged mean $\langle V \rangle$ and $\langle B \rangle$ magnitudes with the related total uncertainties³, number of data points and amplitudes of the light curves, taken from DF04; metal abundances from G04; and reddenings taken from C03.

²According to C03 the fundamental red edge (FRE) of the RR Lyrae stars in DF04 catalogue occurs at $\langle B - V \rangle \sim 0.51$ mag.

³The total photometric errors associated to the mean $\langle V \rangle$ and $\langle B \rangle$ magnitudes are the sum in quadrature of the internal uncertainties, corresponding to the average residuals from the Fourier best fitting models of the observed light curves as computed by GRATIS (GGraphical Analyzer of Time Series, Di Fabrizio 1999, Clementini et al. 2000; see DF04), and of the contributions due to uncertainties of the photometric calibration (0.0175 and 0.032 mag in V and B , respectively, C03 and DF04), and aperture corrections (0.018 and 0.019 mag in V , and 0.032 and 0.014 mag in B , in field A and B, respectively, C03).

3. PULSATION MODELS

In the last few years an extensive and detailed set of updated nonlinear convective pulsation models of RR Lyrae stars has been developed covering wide ranges in period and metal abundances (see Bono et al. 2003, Marconi et al. 2003 and references therein). The physical and numerical assumptions adopted in the theoretical computations were widely discussed in these papers, to which the interested reader is referred for details. We only remark here that thanks to the nonlinearity and the inclusion of convective transfer in a non local, time-dependent approach (see Stellingwerf 1982, Bono & Stellingwerf 1994 for details) current models are able to reproduce all the relevant pulsational observables, namely periods, amplitudes and the complete topology of the instability strip, where the blue boundaries for fundamental and first overtone modes are connected to the position of the H and He ionization regions within the pulsating envelope, whereas the red boundaries are due to the quenching produced by convection, as well as the variations of the relevant quantities (namely luminosity and radial velocity) along the pulsation cycle. The capability to reproduce light and radial velocity curves allows to directly compare observed and predicted variations. We also remind that, as discussed in BCM00, in order to properly reproduce all the morphological features exhibited by the first overtone curves, one needs models constructed by assuming a vanishing overshooting efficiency in the regions where the superadiabatic gradient attains negative values. All the models adopted in the present investigation are computed with this assumption on the treatment of turbulent convection and include an updated input physics (see BCM00 for details).

4. FIT OF THE OBSERVED LIGHT CURVES

In order to reproduce the observed light curves of the selected RR Lyrae stars we adopted as input parameters the metal abundances and the periods reported in Table 1, and for each pulsator we computed isoperiodic model sequences (corresponding to the observed periodicity) for the global metal abundance Z inferred from the empirical $[Fe/H]$ value⁴. Then for each model the theoretical M_V *versus* Phase curve was overimposed to the data, and shifted vertically in magnitude to match the observed behaviour, by allowing at the same time the model input Z to vary within the ranges permitted by the empirical determination. The necessary magnitude shift provides a direct evaluation of the apparent distance modulus of the selected objects.

Although the best fit solution is searched over a wide range of stellar parameters, the stellar masses were selected in order to cover at least the evolutionary predictions for HB stars of the corresponding metal abundances (see e.g. Cassisi et al. 1998, Pietrinferni et al. 2004, D’Antona et al. 2002, Caloi & D’Antona 2005, Sweigart & Catelan 1998, Catelan et al. 1998, Vandenberg et al. 2000). For each adopted stellar mass, the model luminosity and effective temperature were then varied in order to simultaneously reproduce the period and the light curve morphology in the

⁴We adopted the relation $\log Z = [Fe/H] - 1.7$, neglecting the possible occurrence of α enhancement phenomena

V band. To this purpose, for each model, the predicted bolometric light curve was converted into the B, V bands adopting the model atmospheres by Castelli, Gratton & Kurucz (1997a,b). When needed, the standard mixing length value ($l/H_p = 1.5$) was increased up to $l/H_p = 2.2$, again in the range of the values adopted in current evolutionary computations.

The *best fit* models resulting from this investigation are shown in Figs. 1 and 2 for the fundamental mode and the first overtone pulsators separately, and for both V (left panels) and B (right panels) light curves. The corresponding intrinsic stellar parameters, namely the stellar mass, luminosity and effective temperature, are labelled for each pulsator (left panels) and summarized in Table 2, along with the input periods, the adopted global metallicities Z , and mixing length parameter choices. We find that models that best reproduce the V band light curves also show a good agreement with observations in the B band. We also found that models corresponding to the spectroscopic metallicities (transformed to Z values) were generally able to best fit the observed light variations. Only in the case of stars #5902 and #2517 we had to respectively decrease and increase the input empirical metallicity to achieve a good reproduction of the observed light curves. However, these variations were always within the range allowed by the errors of the spectroscopic determinations.

The inferred apparent V and B distance moduli, μ_V and μ_B , and their related uncertainties are reported in Columns 9 and 10 of Table 2, whereas the *pulsational* color excess $E(B - V)$ derived from the difference $\mu_B - \mu_V$ is given in Column 11. True individual V distance moduli μ_0 evaluated from the μ_V values in Column 9 of Table 2 and the adopted reddening values (see Section 4.4) assuming a standard extinction law $A_V = 3.1 * E(B - V)$, are given in Column 12. Finally, in Column 13 we provide the absolute visual magnitudes derived from the model fitting, that is the intensity-averaged mean absolute magnitudes obtained from the best fit model curves in the V band. We note that, since these absolute magnitudes are intrinsic properties of the models, they only depend on the accuracy of the model fitting and of the observed curves, but are completely independent of our knowledge of the variable star reddening and distance.

As shown in Figs. 1 and 2, models are not able to completely reproduce the rising branch of some of the fundamental mode pulsators. This is particularly true for the coolest pulsator in our sample, namely variable star V9660 for which the appearance in the model light curve of a *hump* before the maximum light, changes the slope of the rising branch and causes a delay of the phase of maximum itself. A similar effect is also present, although at lower extent, in the fitting of V2249 and V2525. Analogous problems were found by Castellani et al. (2002) to fit with current pulsation models the fundamental mode RR Lyrae stars at the FRE in the globular cluster ω Cen.

As for the first overtone pulsators, the light curves are found to become close to pure sinusoids as the FOBE is approached (see the case of variable V2119). This behaviour holds for all the explored stellar masses and luminosity levels and might suggest the occurrence of some kind of degeneracy of the solution and the need for fixing a M-L relation. However, since the range of effective temperature covered by almost pure sinusoidal light curves is quite narrow (100-150 K) at each

luminosity level, by selecting the stellar mass in the range of the evolutionary predictions for the adopted metal abundance, the best fit mass and luminosity are constrained by the observed period and amplitude. We note, however, that the very short period, the low apparent luminosity, and the *sinusoidal* light curve of variable V2517 could also make it consistent with a fundamental mode δ Scuti model (with stellar mass in the range 1.5-2.0 M_{\odot}), according to the predictions by Bono et al. (1997).

Finally, we point out that the mixing length parameter adopted to fit the observed light curves has the standard value $l/H_p = 1.5$ for all the first overtone pulsators, whereas it ranges from 1.85 to 2.2 for the fundamental mode variables, again in agreement with previous results from the model fitting technique.

4.1. Uncertainties of the derived intrinsic quantities

In order to evaluate the uncertainties associated to the fitting procedure and their impact on the inferred intrinsic quantities, we have computed additional model sequences for a subsample of fundamental and first overtone pulsators, by varying the stellar parameters around the best fit values. As a result of this procedure we find mean uncertainties of $\delta \log L/L_{\odot} = 0.015$, $\delta \log T_e = 25K$ and $\delta \log M/M_{\odot} = 0.02$. These uncertainties contribute an error of ~ 0.05 mag⁵ in the derived apparent distance moduli μ_V and μ_B . Final errors on μ_V and μ_B should also include the contributions due to the photometric uncertainties of the observed light curves. These are provided in Columns 5 and 8 of Table 1, and once added in quadrature to the 0.05 mag uncertainty of the fitting procedure lead to the total errors associated to the individual μ_V , μ_B values in Columns 9 and 10 of Table 2.

We are aware that the present results hold in the context of the adopted theoretical scenario, namely Bono et al. (2003), and Marconi et al. (2003) pulsation models. However, we note that Bono, Marconi & Stellingwerf (1999) performed a direct comparison with WAS pulsation models. By adopting the same input parameters of WAS for constructing the light curve of the bump Cepheid HV905, they found that predictions by the two hydrocodes, although based on different physical assumptions concerning the input physics and the pulsation/convection interaction, are in reasonable agreement.

Errors on the *pulsational* color excess $E(B-V)$ in Table 2 are computed as the propagation of uncertainties in the μ_V and μ_B values (Columns 9 and 10 of Table 2). Admittedly, they are rather large. Still the *pulsational* reddenings derived for these LMC variables are very reasonable values, and agree well with estimates from other more robust methods (e.g. C03, see Section 4.4), thus providing anyway a sanity check both of other reddening determinations and of the reliability of our model fitting procedure.

⁵This is an average value, the worst model fitting (star #9660) having an uncertainty 0.06 mag.

Finally, errors on the true V distance moduli μ_0 are the sum in quadrature of 3.1 times the uncertainty in the adopted reddenings (see Section 4.4) and of the errors in the apparent μ_V ’s in Column 9 of Table 2. Uncertainties in the M_V ’s instead only depend on the uncertainty of the best fitting procedure (0.05 mag), and on the photometric uncertainties of the observed V light curves (Column 5 of Table 1).

We explicitly note that the smaller errors of the M_V values derived from the model fitting compared to the errors of the μ_0 values reflect the strength of a technique which allows to directly estimate the intrinsic quantity, namely the absolute magnitude of the variable star, without relying upon the knowledge of the reddening, by far one of the most uncertain and controversial quantities in the LMC.

4.2. Comparison with the intrinsic parameters predicted from the evolutionary models

Stellar masses and luminosities derived from the model fitting are generally consistent, within the uncertainties on the model fitting quoted in Sect. 4.1, with the values predicted by stellar evolution models of the proper metal abundances. This is shown in Table 3 where the comparison is made with the evolutionary Zero Age Horizontal Branch (ZAHB) models of Cassisi et al. (1998) and Pietrinferni et al. (2004), D’Antona et al. (2002) and Caloi & D’Antona (2005), Sweigart & Catelan (1998) and Catelan et al. (1998), and finally Vandenberg et al. (2000). The comparison among estimates given by different authors helps us to quantify the uncertainty of current evolutionary predictions. For some of the variables we find that the pulsation model fitting provides significantly smaller masses and/or higher luminosity levels than all the considered ZAHB models, thus suggesting possible evolutionary effects. This is indeed the case for the metal-poor variable stars V5902, V7620, V7477, V2024, and for the metal-intermediate stars V2249, V4179 and V27697. For the relatively metal-rich variable 2517 our pulsational luminosity is slightly fainter than the evolutionary predictions, but consistent with Catelan et al. estimate, within the error. Moreover, as already mentioned, the model metallicity for this star was slightly increased with respect to the spectroscopic value, within the empirical uncertainty. Indeed, a best fit solution was also found for the mean spectroscopic value ($Z=0.002$), however in this case the intrinsic model parameters were not in agreement with the evolutionary predictions. Finally, as noticed in Sect. 4, this star, given the very short period and low apparent luminosity, could also be consistent with a relatively massive fundamental mode δ Scuti pulsator.

4.3. Comparison with the intrinsic parameters from the Fourier decomposition of the light curves

In Table 4 we have summarized masses, luminosities, effective temperatures, and absolute magnitudes derived from the present study and, for comparison, the same quantities as estimated by DF04 from the Fourier parameters of the visual light curves for the variables in the present sample for which this analysis was possible, namely 5 RRab’s that satisfy Jurcsik & Kovács (1996) *compatibility conditions* (see details in Section 6 of DF04).

We note that while masses estimated from the two methods agree within a few hundreds, luminosities and effective temperatures from the model fitting are on average systematically larger, respectively by 0.07 dex and 200 K, than the corresponding quantities from the Fourier analysis. These systematic effects seem to suggest the occurrence of problems with the calibration of Fourier parameters, making them still not reliable (see also the discussion in Cacciari et al. 2004).

Moreover, the absolute magnitudes from the model fitting span an interval about 0.13 mag larger than those from the Fourier parameters, a similar result was also found by DF04.

4.4. Comparison of reddening estimates

The amount of reddening affecting the LMC still remains poorly known since estimates by different techniques and authors have often provided controversial results that do not agree to each other (see U99, Zaritsky 1999, C03, A04, Zaritsky et al. 2004). The LMC color excess is also found to vary by large amounts from one region of the galaxy to the other, thus requiring local estimates that are to be preferred to the use of average values over large areas. The *pulsational* reddenings, being derived for each star individually, indeed provide estimates of the *local* reddening in the region containing the variable, that can be directly compared to other *local* estimates of the $E(B - V)$.

In Table 5 the *pulsational* reddenings derived from the model fittings are compared with estimates obtained for the same stars or LMC regions by C03, U99, and A04 using different techniques. In particular, reddenings labelled “strip” (see Column 4 of Table 5) were obtained by C03 from the comparison of the colors of the edges of the RR Lyrae instability strip defined by the variables contained in the two LMC fields they observed, with those of the low reddening globular cluster M3. They determined two distinct values, that apply to the variables contained in each given field, separately. Reddenings labelled “Sturch” (see Column 5 of Table 5) are “individual” estimates derived by C03 using Sturch (1966) method, which is based on the color at minimum light of the fundamental mode RR Lyrae stars. U99 is the average reddening measured from variations in the I luminosity of clump stars located in OGLE-II field LMC_SC21. This field partially overlaps to C03 Field A, and according to Table 14 of DF04, two of the variable stars analyzed here (namely the RRC stars #2119 and #27697) fall into the common region.

Finally, A04 is the mean color excess estimated from 330 first overtone RR Lyrae stars spread over 16 MACHO fields close to the LMC bar. We only have the RRc star #8837 in common with A04 sample (see Table 12 in that paper).

As discussed in Section 4, notwithstanding their large uncertainties, the *pulsational* reddenings provide a consistency check of the color excesses derived by other techniques. In this respect we note that they agree well with the empirical values by C03 while, on average, are about 0.02-0.03 mag smaller than U99 and A04 estimates. However, this systematic difference is not surprising given the rather clumpy reddening of the LMC, the larger areas covered by the reddening indicators used in both U99⁶ and A04, and their locations on or closer to the LMC bar than in C03.

In the following we will adopt for each of our targets the weighted average of the *pulsational*, C03-strip, and C03-Sturch reddenings (values in Columns 3,4 and 5 of Table 5). These average values are provided in Column 8 with their related uncertainties that are simply the standard deviations of the weighted means. They will be used together with the apparent distance moduli μ_V in Table 2 to derive true distance moduli μ_0 for each of our targets (see Section 5).

5. THE DISTANCE TO THE LMC

True distance moduli μ_0 for our program stars were computed from the apparent moduli in Column 9 of Table 2 and the reddenings in Column 8 of Table 5 using the standard extinction law ($A_V=3.1 \times E(B-V)$). They are provided in Column 12 of Table 2. Errors in these μ_0 values are the sum in quadrature of the uncertainties in the apparent distance moduli μ_V and 3.1 times the uncertainty of the reddenings. By performing a weighted mean of these μ_0 values we obtain a final estimate for the true distance modulus of the LMC of $\langle \mu_0 \rangle = 18.54 \pm 0.02$ ($\sigma=0.09$, standard deviation about the average of the 14 RR Lyrae stars). The 0.09 mag dispersion of this average value is fully accounted for by uncertainties in the reddening and model fitting technique, implying that the distance moduli derived for individual objects are consistent within the respective error bars.

The derived LMC average distance modulus is well in the range of the most recent evaluations in the literature that all prefer the *long* distance scale (see Walker 2003, C03, Alves 2004, and reference therein), agrees well with the results of the light curve fitting of two Classical Cepheids in the LMC by BCM02, and is in excellent agreement with Keller & Wood (2002) LMC distance modulus from the model fitting of 20 LMC *bump* Cepheids. This excellent agreement between Population I and II distance indicators in the LMC is very rewarding in light of the longstanding controversy existing in the past on the distance to the LMC based on these two independent indicators. Moreover the agreement with Keller & Wood determination, which is based on a different pulsation code and

⁶The common area with C03 Field A is less than 10% of OGLE-II field LMC_SC21, that extents both more inside and outside the LMC bar.

relies on different physical and numerical assumptions, supports the soundness and reliability of our results.

We also point out that a different choice for the reddening, namely adoption of U99 and A04 average values ($E(B - V) = 0.142$ mag) would give $\langle \mu_0 \rangle = 18.46 \pm 0.02$, again in the range of the “long” scale and at odds with methods favoring much shorter distance moduli (in the range from ~ 18.2 to ~ 18.3 mag) for the LMC (e.g. Fernley et al. 1998a, Udalski 2000, Popowski 2000, Dambis 2004, Rastorguev, Dambis, & Zabolotskikh 2004).

5.1. The RR Lyrae luminosity-metallicity relation

HB and RR Lyrae stars are known to follow a luminosity-metallicity relation generally considered to be of linear form. The slope of this relation is still matter of debate with values in the range from 0.30 (Sandage 1993) to 0.18-0.20 mag/dex (Caloi et al. 1997, Cassisi et al. 1998, Fernley et al. 1998b, C03, G04, Rich et al. 2001, 2005). There are also empirical and theoretical evidences for a non-linearity of the relation followed by the Galactic globular clusters (Caputo et al. 2000, Rey et al. 2000), however there is no clear proof of such a non-linearity in the behaviour of the Galactic (Fernley et al. 1998b) and LMC (C03, G04) field RR Lyrae stars, as well as in the M31 globular clusters (Rich et al. 2001, 2005). At fixed metal abundance there is also an intrinsic spread in the HB luminosity, due to evolutionary effects, (see e.g. Sandage 1990). Such evolutionary effects are also predicted by evolutionary and synthetic horizontal branch computations (see e.g. Lee, Demarque & Zinn 1990, Caputo et al. 1993, Caloi et al. 1997, Cassisi et al. 2004 and references therein). A fairly large number of objects should be considered in order to reduce the impact of the evolutionary effects, since evolution off the ZAHB can affect the slope of the luminosity-metallicity relation.

C03 and G04 have recently derived the slope of the luminosity-metallicity of the LMC RR Lyrae stars using a fairly significant large sample of variables (98 stars) based on their homogeneous and accurate photometric and spectroscopic datasets for these stars. Since RR Lyrae stars in the LMC can in the first approximation all be considered at the same distance from us, C03 and G04 used directly the dereddened apparent visual magnitudes of the variables without any assumption on their absolute magnitudes, that might be affected by problems of zero point in the distance scale. Further advantages of C03 and G04 approach were the significant statistics of their sample, and the large number of objects at intermediate metal abundance: the metal distribution of C03 and G04 sample peaks at $[\text{Fe}/\text{H}] = -1.48$ dex, with the bulk of stars (66 objects) in the metallicity bin $-1.7 < [\text{Fe}/\text{H}] < -1.3$. Both these characteristics allow minimization of the effects on the slope of the intrinsic spread in luminosity of the RR Lyrae stars due to their evolution off the ZAHB. They derived a rather mild slope of 0.214 ± 0.047 mag/dex in agreement with results from the Baade-Wesselink method of 28 Galactic field RR Lyrae stars ($\Delta M_V / [Fe/H] = 0.20 \pm 0.04$ mag/dex, Fernley et al. 1998b), and from the HB luminosity of 20 globular clusters in the Andromeda galaxy ($\Delta M_V / [Fe/H] = 0.20$ mag/dex ± 0.09 , Rich et al. 2005).

We have combined the $\langle M_V \rangle$ values derived from the model fitting (see Column 13 of Table 2) with the metallicities used in the fitting (see Column 4 of Table 2) to determine the slope of the luminosity-metallicity relation defined by the 14 LMC RR Lyrae stars in our sample. A simple linear fit provides a slope of $\Delta M_V/[Fe/H]=0.34$ mag/dex using all objects and of 0.28 mag/dex if star # 2517, the object with rather unusually faint absolute magnitude, is discarded. The same linear regression using the corresponding dereddened apparent magnitudes V_0 (obtained from the average $\langle V \rangle$ values in Column 4 of Table 1 corrected for the reddenings in Column 8 of Table 5 assuming the standard extinction law) would give $\Delta M_V/[Fe/H]=0.31$ and 0.24, respectively. All these values are higher than the slope derived by C03 and G04. However, since the V_0 *versus* $[Fe/H]$ fit also provides steeper slopes compared to C03 and G04 value, this demonstrates that the difference is due to the sample selection, and that it does not arise from errors in the absolute magnitudes obtained by the model fitting. Indeed, it should be kept in mind that the 14 LMC RR Lyrae stars analyzed in this paper represent less than 15% of C03 and G04 sample, and that although the peak of the fit metallicities of our RR Lyrae subsample ($[Fe/H]_{fit}=-1.53$) is very close to the average metallicity of C03 and G04 total sample, our metallicity distribution is more unbalanced towards low metal abundances. Moreover, the comparison with the ZAHB evolutionary predictions indicates the presence of evolutionary effects for almost all the metal poor objects in our sample, and these effects are expected to cause a steepening of the slope. Thus the higher slopes found here are simply the result of both the poorer statistics and the higher incidence of evolutionary effects in our sample compared to C03 and G04 one.

6. SUMMARY AND FINAL REMARKS

We have fitted the nonlinear convective pulsation models by Bono et al. (2003) and Marconi et al. (2003) to 14 LMC RR Lyrae stars with accurate photometry, metal abundances, and reddening estimates by DF04, G024 and C03. This is the first time that the model fitting technique is applied to a significantly large number of RR Lyrae stars within the same stellar system, thus providing an important assessment of the predictive capabilities of the adopted theoretical pulsation models and, at the same time, a new independent estimate of the Population II distance to this fundamental first step of the astronomical distance ladder.

We have obtained $\mu_0(LMC)=18.54 \pm 0.02$ in very good agreement with the LMC “long” astronomical distance (Walker 2003, C03, Alves 2004).

Masses, luminosities, and effective temperatures derived from the model fitting are in satisfactory agreement with the predictions of theoretical HB models, as derived from various authors in the literature. We notice that such a detailed and punctual comparison between the results of pulsation model fitting and the evolutionary expectations had never been performed in the previous applications of the method to RR Lyrae stars.

The *pulsational* reddenings are in good agreement with values in C03, thus further supporting

the estimates in that paper, and the soundness of the present approach.

Finally we remind that our final result for the LMC distance modulus is in excellent agreement with the estimate provided by Keller & Wood (2002) on the basis of a similar method applied to 20 Classical Cepheids in the same stellar system. This occurrence suggests that the results of the model fitting technique are only marginally dependent on the adopted pulsation code, as well as on the physical and numerical assumptions in the model computations. It also shows that there is no discrepancy between the Population I and Population II distance scales to the Large Magellanic Cloud.

We warmly thank Santi Cassisi, Marcio Catelan and Don Vandenberg for providing us their ZAHB models in electronic forms. A special thanks goes to Vittoria Caloi and Franca D’Antona for sending us their evolutionary models in advance of publication and for specifically computing some of the ZAHBs used in the comparison with the evolutionary models. It is a pleasure to thank Franco Zavatti for many enlightening discussions on the regression line routines used in astronomy, and the anonymous referee for useful comments. Financial support for this study was provided by INAF Progetti di Ricerca di Interesse Nazionale under the scientific project “Stars and Clusters as Tracers of the LMC Structure and Evolution” (P.I.: G. Bertelli), and by MIUR, under the scientific projects “Stellar Populations in the Local Group” (P.I.: Monica Tosi) and “Continuity and Discontinuity in the Milky Way Formation” (P.I.: Raffaele Gratton).

REFERENCES

- Alcock, C., et al. 2004, *AJ*, 127, 334 (A04)
- Alves, D.R. 2004, *New Astronomy Reviews*, Volume 48, Issue 9, pages 659-665 (astro-ph/0310673)
- Blazhko, S. 1907, *Astron. Nachr.*, 175, 325
- Bono, G., Castellani, V., & Marconi, M. 2000, *ApJ*, 532, L129 (BCM00)
- Bono, G., Castellani, V., & Marconi, M. 2002, *ApJ*, 565, L83 (BCM02)
- Bono, G., Marconi, M., & Stellingwerf 1999, *ApJS*, 122, 167
- Bono, G., Caputo, F., Cassisi, S., Castellani, V., Marconi, M., & Stellingwerf, R.F. 1997, *ApJ*, 477, 346
- Bono, G., Caputo, F., Castellani, V., Marconi, M., Storm, J., & Degl’Innocenti, S. 2003, *MNRAS*, 344, 1097
- Bono, G., & Stellingwerf, R.F. 1994, *ApJS*, 93, 233
- Cacciari, C. 1999, in *ASP Conf. Ser.* 167, *Harmonizing Cosmic Distance Scales in a Post-Hipparcos Era*, ed. D. Egret, & A. Heck (San Francisco: ASP), 140
- Cacciari, C., Corwin, T.M., & Carney, B.W. 2004, *AJ*, in press (astro-ph/0409567)
- Caloi, V., D’Antona, F., & Mazzitelli, I. 1997, *A&A*, 320, 823
- Caloi, V., & D’Antona, F. 2005, private communication
- Caputo, F., De Rinaldis, A., Manteiga, M., Pulone, L., & Quarta, M.L. 1993, *A&A*, 276, 41
- Caputo, F., Castellani, V., Marconi, M., & Ripepi, V. 2000, *MNRAS*, 316, 819
- Cassisi, S., Castellani, V., Degl’Innocenti, S., & Weiss, A. 1998, *A&AS*, 129, 627
- Cassisi, S., Castellani, M., Caputo, F., S., & Castellani, V. 2004, *A&A*, 426, 641
- Carretta, E., Gratton, R.G., Clementini, G., & Fusi Pecci, F. 2000, *ApJ*, 533, 215
- Castellani, V., Degl’Innocenti, S., & Marconi, M. 2002, in *ASP Conf. Ser.* 265, *Omega Centauri, A Unique Window into Astrophysics*, ed. F. van Leeuwen, J. D. Hughes, & G. Piotto (San Francisco: ASP), 193
- Castelli, F., Gratton, R.G., & Kurucz 1997a, *A&A*, 318, 841
- Castelli, F., Gratton, R.G., & Kurucz 1997b, *A&A*, 324, 432
- Catelan, M., Borissova, J., Sweigart, A.V., & Spassova, N. 1998, *ApJ*, 494, 265
- Clementini, G., et al. 2000, *AJ*, 120, 2054
- Clementini, G., Gratton, R.G., Bragaglia, A., Carretta, E., Di Fabrizio, L., & Maio, M. 2003, *AJ*, 125, 1309 (C03)
- Dambis, A.K. 2004, in *EAS Publications Series, Galactic Dynamics*, ed. C. Boily, P. Patsis, C. Theis, S. Portegies Zwart, & R. Spurzem, (EDP Science 2004), in press (astro-ph/0303463)

- D’Antona, F., Caloi, V., Montalbán, J., Ventura, P., & Gratton, R. 2002, *A&A*, 395, 69
- Di Criscienzo, M., Marconi, M., & Caputo, F. 2004, *ApJ*, 612, 1092
- Di Fabrizio, L. 1999, Laurea Degree Thesis, University of Bologna
- Di Fabrizio, L., et al. 2002, *MNRAS* 336, 841
- Di Fabrizio, L., Clementini, G., Maio, M., Bragaglia, A., Carretta, E., Gratton, R.G., Montegriffo, P., & Zoccali, E. 2004, *A&A*, in press (DF04, astro-ph/0409758)
- Freedman, W.L., et al. 2001, *ApJ*, 553, 47
- Fernley, J.A., Barnes, T.G., Skillen, I., Hawley, S.L., Hanley, C.J., Evans, D.W., Solano, E., & Garrido, R. 1998a, *A&A*, 330, 515
- Fernley, J.A., Carney, B.W., Skillen, I., Cacciari, C., & Janes, K. 1998b, *MNRAS*, 293, L61
- Gratton R.G., Bragaglia, A., Clementini, G., Carretta, E., Di Fabrizio, L., Maio, M., & Taribello, E. 2004, *A&A*, 421, 937 (G04)
- Harris, W.E. 1996, *AJ*, 112, 1487
- Jurcsik, J., & Kovács, G. 1996, *A&A*, 312, 111
- Keller, S.C., & Wood, P.R. 2002, *ApJ*, 578, 144
- Lee, Y.W., Ddemarque, P., & Zinn, R. 1990, *ApJ*, 350, 155
- Marconi, M., Caputo, F., Di Criscienzo, M., & Castellani, M. 2003, *ApJ*, 596, 299
- Pietrinferni, A., Cassisi, S., Salaris, M., & Castelli, F. 2004, *ApJ*, 612, 168
- Popowski, P. 2000, *ApJ*, 528, L9
- Rastorguev, A.S., Dambis, A.K., & Zabolotskikh, M.V. 2004, in *The three Dimensional Universe with GAIA*, Paris-Meudon, in press
- Rey, S-C., Lee, Y-W., Joo, J-M., Walker, A., & Baird, S. 2000, *AJ*, 119, 1824
- Rich, R.M., Corsi, C.E., Bellazzini, M., Federici, L., Cacciari, C., & Fusi Pecci, F. 2001, in *Extragalactic Star Clusters*, ed. E.K. Grebel, D. Geisler, & D. Minniti (San Francisco:ASP, IAU Symp., 207, 140
- Rich, R.M., Corsi, C.E., Cacciari, C., Federici, L., Fusi Pecci, F., Djorgovski, S.G., & Freedman W. 2005, *AJ*, submitted
- Sandage, A. 1990, *ApJ*, 350, 603
- Sandage, A. 1993, *AJ*, 106, 703
- Stellingwerf, R.F. 1982, *ApJ*, 262, 330
- Sturch, C. 1966, *ApJ*, 143, 774
- Sweigart, A.V., & Catelan, M. 1998, *ApJ*, 501, L63
- Tammann, G.A., Sandage, A., & Reindl, B. 2003, *A&A*, 404, 423

- Udalski, A. 2000, *ApJ*, 531, L25
- Udalski, A., Szymański, M., Kubiak, M., Pietrzyński, G., Soszyński, I., Woźniak, P., & Zebrunń, K. 1999, *Acta Astron.*, 49, 201 (U99)
- VandenBerg, D.A., Swenson, F.J., Rogers, F.J., Iglesias, C.A. & Alexander, D.R. 2000, *ApJ*, 532, 430
- Walker, A.R. 1999, in *Astrophysics and Space Science Library 237, Post-Hipparcos Cosmic Candles*, ed. A. Heck, & F. Caputo, (Kluwer Academic Publishers), 125
- Walker, A.R. 2003, in *Lecture Notes in Physics 635, Stellar Candles for the Extragalactic Distance Scale*, ed. D. Alloin, & W. Gieren, (Berlin:Springer), 265
- Wood, P.R., Arnold, A., & Sebo, K.M. 1997, *ApJ*, 485, L52 (WAS)
- Zaritsky, D. 1999, *AJ*, 118, 2824
- Zaritsky, D., Harris, J., Thompson, I.B., & Grebel, E.K. 2004, *AJ*, in press (astro-ph/0407006)
- Zinn, R., & West, M.J. 1984, *ApJS*, 55, 45

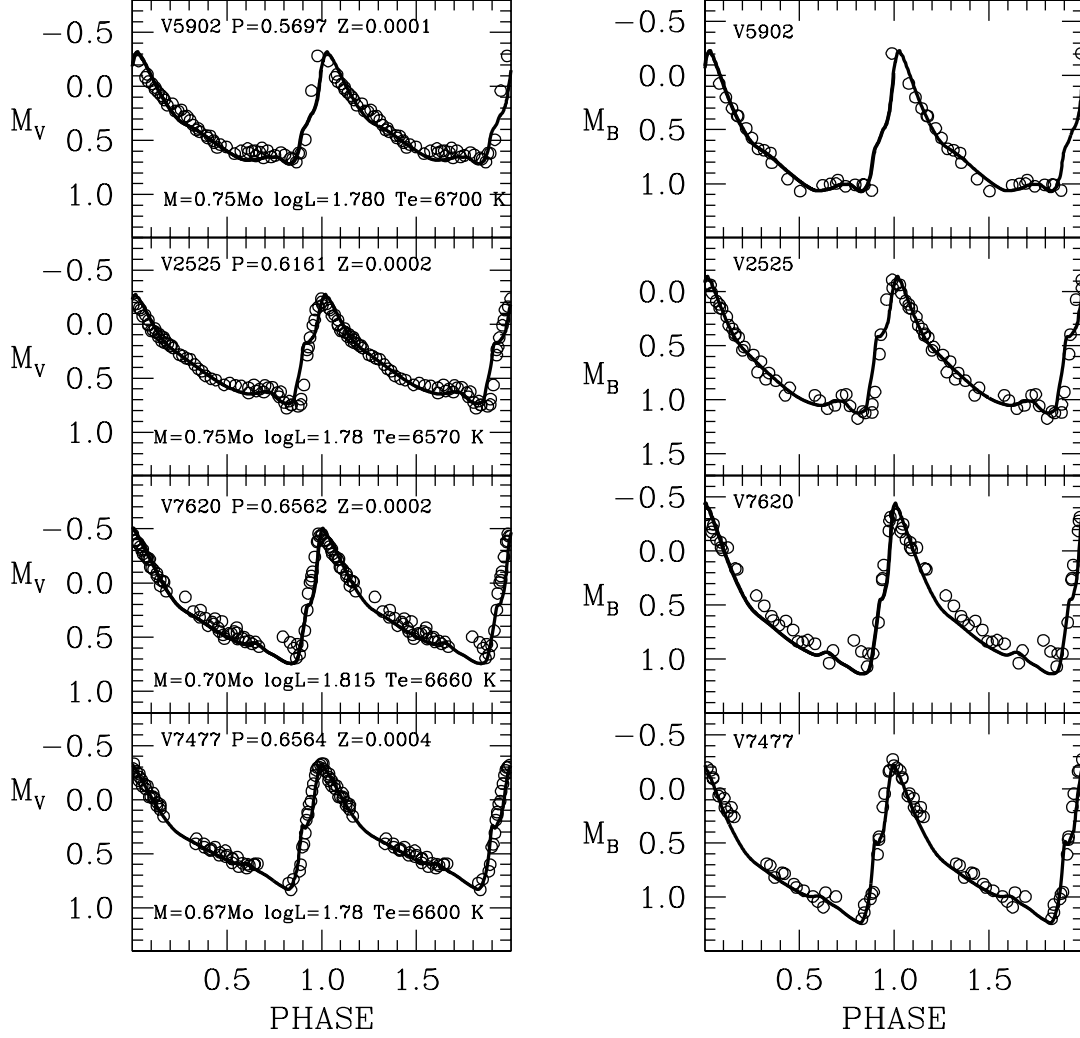


Fig. 1.— Results from the theoretical modelling of the V (left panels) and B (right panels) light curves of the fundamental mode pulsators in our sample. Stars are ordered by increasing metallicity. For each variable we indicate the star identifier and period according to DF04, the global metal abundance Z inferred from the $[\text{Fe}/\text{H}]$ values in G04 or DF04, and the mass, luminosity and effective temperature obtained from the fit.

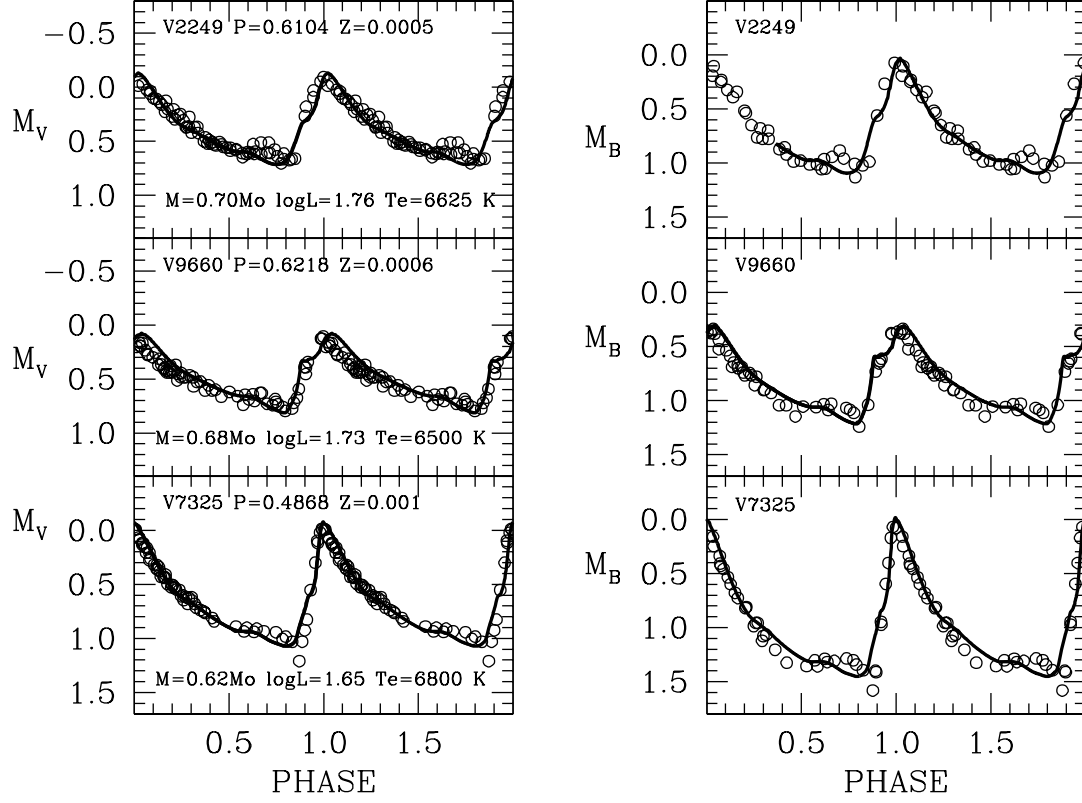


Fig. 1 – continued –

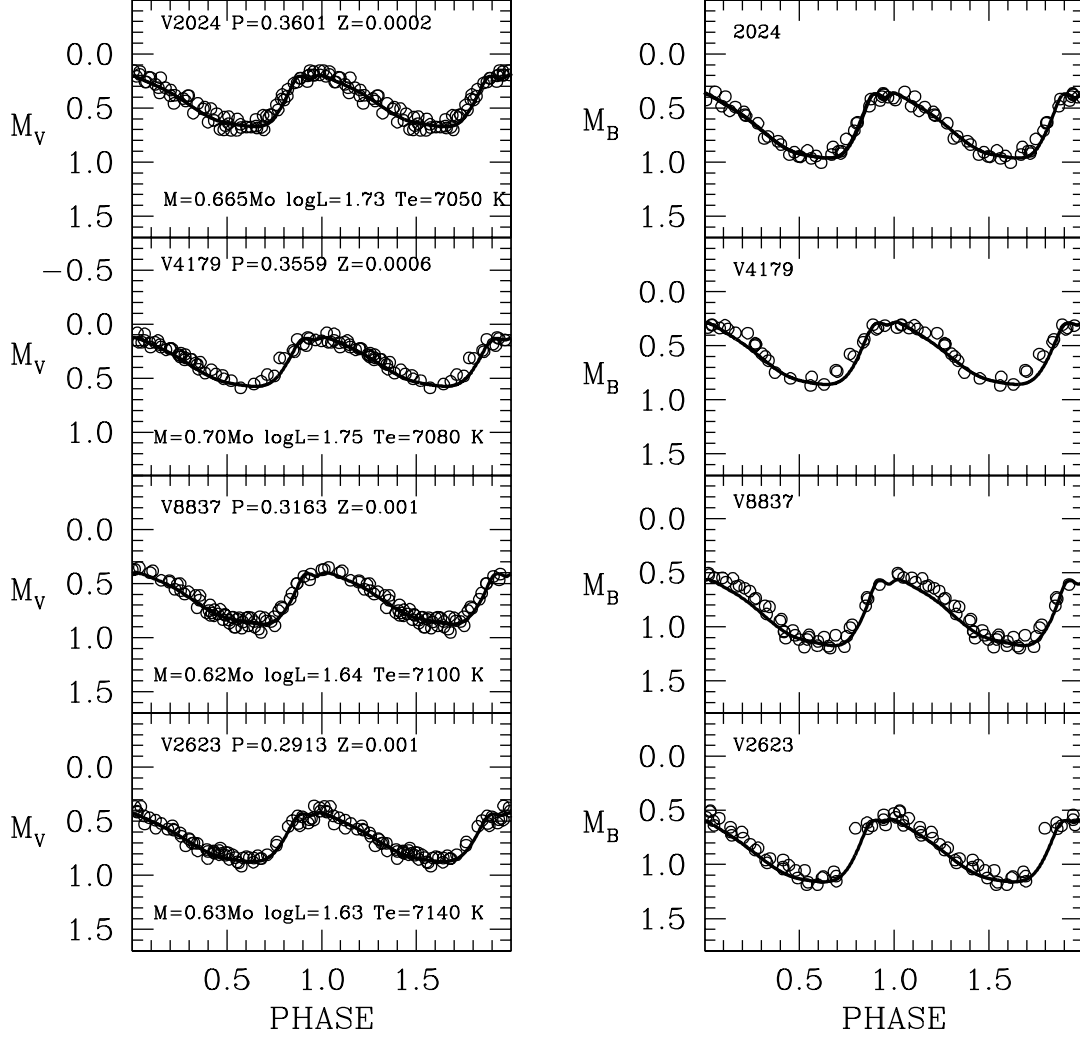


Fig. 2.— Results from the theoretical modelling of the V (left panels) and B (right panels) light curves of the first overtone pulsators in our sample. Stars are ordered by increasing metallicity. For each variable we indicate the star identifier and period according to DF04, the global metal abundance Z inferred from the $[\text{Fe}/\text{H}]$ values in G04 or DF04, and the mass, luminosity and effective temperature obtained from the fit.

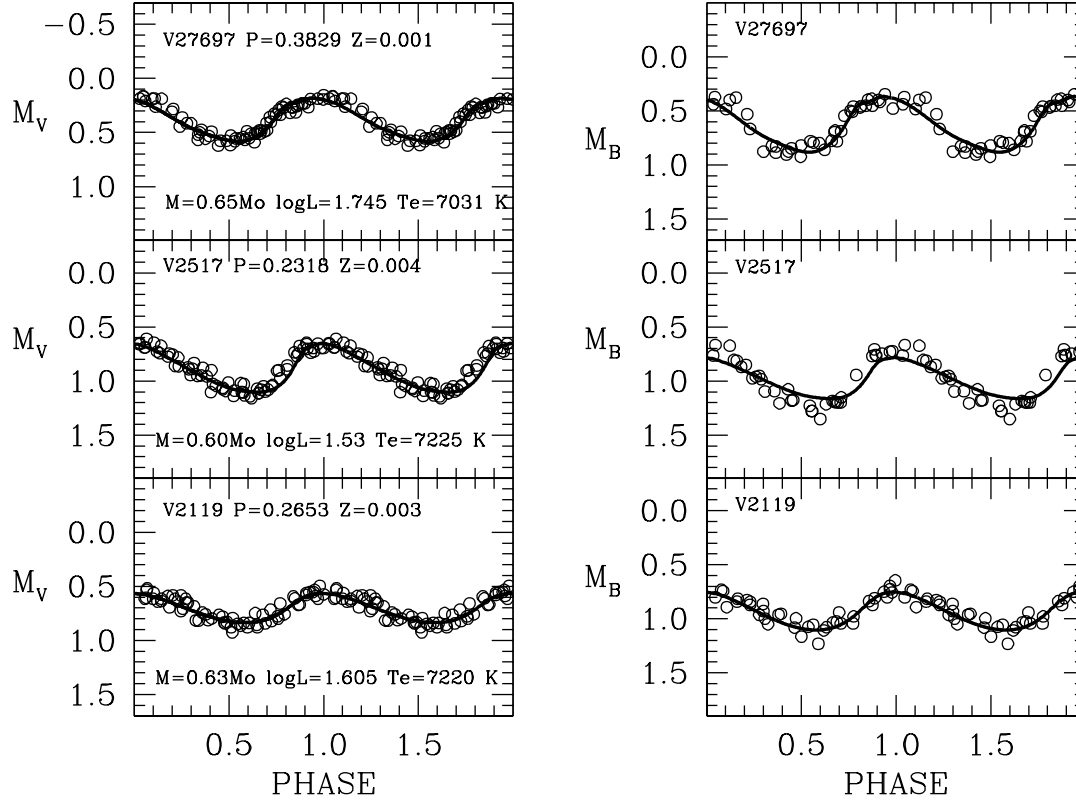


Fig. 2 – continued –

Table 1: Observed characteristics of the program stars

Star ^a	type ^a	P ^a day	$\langle V \rangle^a$ mag	σ_V mag	N _p V	$\langle B \rangle^a$ mag	σ_B mag	N _p B	A _V ^a mag	A _B ^a mag	[Fe/H] ^b
5902	ab	0.570	19.121	0.033	54	19.472	0.037	23	1.015	1.282	-2.12 ± 0.11
2525	ab	0.616	19.340	0.036	69	19.764	0.063	41	0.991	1.272	-2.06 ± 0.14
7620	ab	0.656	19.079	0.040	70	19.409	0.067	37	1.071	1.366	-2.05 ± 0.12
7477	ab	0.656	19.183	0.033	69	19.552	0.057	40	1.108	1.371	-1.67 ± 0.28
2249	ab	0.610	19.346	0.041	69	19.775	0.052	35	0.747	0.987	-1.56 ± 0.15
9660	ab	0.622	19.392	0.038	67	19.862	0.054	41	0.669	0.811	-1.50 ± 0.20
7325	ab	0.487	19.435	0.035	68	19.845	0.054	40	1.131	1.449	-1.28 ± 0.09
2024	c	0.360	19.500	0.048	72	19.876	0.059	40	0.509	0.606	-1.92 ± 0.14
4179	c	0.356	19.173	0.037	50	19.502	0.048	29	0.438	0.560	-1.53 ± 0.27
8837	c	0.316	19.566	0.045	64	19.905	0.059	41	0.501	0.631	-1.52 ± 0.22
2623	c	0.291	19.368	0.043	65	19.631	0.064	40	0.441	0.595	-1.34 ± 0.30
27697	c	0.383	19.166	0.041	66	19.541	0.064	39	0.396	0.471	-1.33 ± 0.25
2517	c	0.232	19.695	0.049	69	19.925	0.052	36	0.452	0.555	-0.92 ± 0.33
2119	c	0.265	19.659	0.052	64	19.986	0.071	39	0.297	0.354	-0.79 ± 0.26

^a Star identifier, type, period, intensity-averaged mean magnitudes with the related uncertainties, number of data points, and amplitudes of the light variations are from DF04

^b Metallicities [Fe/H] are on G04 metallicity scale.

Table 2: Intrinsic parameters, distance moduli, reddenings and absolute magnitudes derived from the modelling of the light curves

Star	type	P day	Z^a	l/H_p	M/M_\odot	$\log L/L_\odot$	T_e K	μ_V mag	μ_B mag	$E(B - V)$ mag	μ_0 mag	$< M_V >$ mag
5902	ab	0.570	0.0001	2.1	0.75	1.78	6700	18.81±0.060	18.87±0.062	0.06±0.086	18.519±0.080	0.347±0.060
2525	ab	0.616	0.0002	1.9	0.75	1.78	6750	18.99±0.062	19.12±0.080	0.13±0.101	18.562±0.130	0.336±0.062
7620	ab	0.656	0.0002	1.89	0.70	1.815	6660	18.87±0.064	18.97±0.084	0.10±0.106	18.579±0.074	0.252±0.064
7477	ab	0.656	0.0004	1.85	0.67	1.78	6600	18.89±0.060	18.99±0.076	0.10±0.096	18.515±0.069	0.336±0.060
2249	ab	0.610	0.0005	2.2	0.70	1.76	6625	18.99±0.065	19.12±0.072	0.13±0.097	18.658±0.121	0.392±0.065
9660	ab	0.622	0.0006	2.0	0.68	1.73	6500	18.89±0.063	19.03±0.074	0.14±0.097	18.549±0.073	0.467±0.063
7325	ab	0.487	0.001	2.0	0.62	1.65	6800	18.79±0.061	18.89±0.074	0.10±0.096	18.437±0.062	0.640±0.061
2024	c	0.360	0.0002	1.5	0.665	1.73	7050	19.08±0.069	19.21±0.077	0.13±0.103	18.720±0.076	0.435±0.069
4179	c	0.356	0.0006	1.5	0.70	1.75	7080	18.85±0.062	18.96±0.069	0.11±0.093	18.580±0.082	0.348±0.062
8837	c	0.316	0.001	1.5	0.62	1.64	7100	18.95±0.067	19.06±0.077	0.11±0.102	18.590±0.068	0.637±0.067
2623	c	0.291	0.001	1.5	0.63	1.63	7140	18.73±0.066	18.80±0.081	0.07±0.104	18.374±0.122	0.652±0.066
27697	c	0.383	0.001	1.5	0.65	1.745	7031	18.80±0.065	18.93±0.081	0.13±0.104	18.440±0.072	0.376±0.065
2517	c	0.232	0.004	1.5	0.60	1.53	7225	18.825±0.070	18.965±0.072	0.14±0.100	18.552±0.137	0.889±0.070
2119	c	0.265	0.003	1.5	0.63	1.605	7220	18.96±0.072	19.06±0.087	0.10±0.113	18.600±0.080	0.705±0.072

^a Z values were derived from the observed metal abundances $[\text{Fe}/\text{H}]$ in Table 1 using the relation $\log Z = [Fe/H] - 1.7$

Table 3: Comparison with the evolutionary masses and luminosities predicted by different sets of ZAHB models

Star	type	P day	Z	$\log T_e$ Puls.	M Puls.	M C98/P04	M DC02/05	M SC98	M V00	$\log L$ Puls.	$\log L$ C98	$\log L$ DC02/05	$\log L$ SC98	$\log L$ V00
5902	ab	0.570	0.0001	3.826	0.75	0.84	0.84	—	0.80	1.78	1.79	1.79	—	1.75
2525	ab	0.616	0.0002	3.818	0.75	0.76	0.77	—	0.74	1.78	1.75	1.75	—	1.72
7620	ab	0.656	0.0002	3.823	0.70	0.76	0.76	—	0.74	1.815	1.75	1.75	—	1.72
7477	ab	0.656	0.0004	3.819	0.67	—	—	—	0.69	1.78	—	—	—	1.70
2249	ab	0.610	0.0005	3.821	0.70	—	—	0.68	0.67	1.76	—	—	1.67	1.68
9660	ab	0.622	0.0006	3.813	0.68	—	—	—	0.66	1.73	—	—	—	1.68
7325	ab	0.487	0.001	3.833	0.62	0.66	0.65	0.64	0.63	1.65	1.69	1.68	1.63	1.65
2024	c	0.360	0.0002	3.848	0.665	0.75	0.75	—	0.72	1.73	1.73	1.74	—	1.71
4179	c	0.356	0.0006	3.850	0.70	—	—	—	0.65	1.75	—	—	—	1.67
8837	c	0.316	0.001	3.851	0.62	0.65	0.65	0.65	0.63	1.64	1.68	1.67	1.63	1.65
2623	c	0.291	0.001	3.854	0.63	0.65	0.645	0.65	0.63	1.63	1.68	1.67	1.63	1.65
27697	c	0.383	0.001	3.847	0.65	0.66	0.645	0.65	0.63	1.74	1.68	1.67	1.63	1.65
2517	c	0.232	0.004	3.859	0.60	0.59	0.59	0.59	0.575	1.53	1.61	1.59	1.55	1.58
2119	c	0.265	0.003	3.858	0.63	0.61	—	—	0.59	1.61	1.62	—	—	1.60

Notes: Puls. = *pulsational*, present paper; C98/P04 = Cassisi et al. (1998), and Pietrinferni et al. (2004); DC02/05= D’Antona et al. (2002), and Caloi & D’Antona (2005); SC98 = Sweigart & Catelan (1998), and Catelan et al. (1998); V00 = VandenBerg et al. (2000)

Masses and luminosities are in solar units.

Table 4: Comparison with the intrinsic parameters derived from the Fourier decomposition of the light curve of the fundamental mode pulsators

Star	type	P day	M/M_{\odot}	M/M_{\odot} Fourier	$\log L/L_{\odot}$	$\log L/L_{\odot}$ Fourier	T_e	T_e Fourier	$< M_V >$	$< M_V >$ Fourier
5902	ab	0.570	0.75	0.71	1.78	1.68	6700	6471	0.347 ± 0.060	0.531 ± 0.027
2525	ab	0.616	0.75	0.69	1.78	1.69	6570	6397	0.336 ± 0.062	0.513 ± 0.027
2249	ab	0.610	0.70	0.73	1.76	1.69	6625	6397	0.392 ± 0.065	0.520 ± 0.027
9660	ab	0.622	0.68	0.66	1.73	1.67	6500	6310	0.467 ± 0.063	0.580 ± 0.026
7325	ab	0.487	0.62	0.66	1.65	1.61	6800	6561	0.640 ± 0.061	0.684 ± 0.028

Notes: Stars #2249 and #9660 have large Dm values: $Dm \leq 4.769$ and $Dm \leq 3.746$, respectively (see Sect. 6 in DF04).

Table 5: Comparison of the reddening values

Star	type	$E(B-V)$ mag <i>Pulsational</i>	$E(B-V)$ mag C03(strip)	$E(B-V)$ mag C03(Sturch)	$E(B-V)$ mag U99 (1)	$E(B-V)$ mag A04 (2)	$< E(B-V) >$ mag Adopted (3)
5902	ab	0.06 ± 0.086	0.086 ± 0.017	0.108	—	—	0.094 ± 0.017
2525	ab	0.13 ± 0.101	0.116 ± 0.017	0.169	—	—	0.138 ± 0.037
7620	ab	0.10 ± 0.106	0.086 ± 0.017	0.104	—	—	0.094 ± 0.012
7477	ab	0.10 ± 0.096	0.116 ± 0.017	0.130	—	—	0.121 ± 0.011
2249	ab	0.13 ± 0.097	0.086 ± 0.017	0.134	—	—	0.107 ± 0.033
9660	ab	0.14 ± 0.097	0.116 ± 0.017	0.100	—	—	0.110 ± 0.012
7325	ab	0.10 ± 0.096	0.116 ± 0.017	0.112	—	—	0.114 ± 0.004
2024	c	0.13 ± 0.103	0.116 ± 0.017	—	—	—	0.116 ± 0.010
4179	c	0.11 ± 0.093	0.086 ± 0.017	—	—	—	0.087 ± 0.017
8837	c	0.11 ± 0.102	0.116 ± 0.017	—	—	0.140	0.116 ± 0.004
2623	c	0.07 ± 0.104	0.116 ± 0.017	—	—	—	0.115 ± 0.033
27697	c	0.13 ± 0.104	0.116 ± 0.017	—	0.144 ± 0.02	—	0.116 ± 0.010
2517	c	0.14 ± 0.100	0.086 ± 0.017	—	—	—	0.088 ± 0.038
2119	c	0.10 ± 0.113	0.116 ± 0.017	—	0.144 ± 0.02	—	0.116 ± 0.011

Notes: (1) U99 reddening is the average value over the entire field OGLE-II LMC_SC21, that includes about 40% of C03 Field A; (2) A04 color excess is the average values from 330 RRc stars spread over 16 MACHO fields close to the LMC bar; (3) weighted average of *pulsational*, C03(strip) and C03(Sturch) reddenings.